Effect of frequency chirping on supercontinuum generation in photonic crystal fibers

Zhaoming Zhu and Thomas G. Brown

The Institute of Optics and Laboratory for Laser Energetics, University of Rochester, Rochester, New York 14627, USA

zzhu@optics.rochester.edu

Abstract: Pre-chirp of the input pulse has a significant effect on pulse evolution in a photonic crystal fiber. We present numerical simulations which show that the supercontinuum bandwidth increases with the linear chirp, and that the coherence of supercontinuum improves as frequency chirping increases. An optimal positive chirp is identified that maximizes the supercontinuum bandwidth, corresponding to the formation of only one red-shifting Raman soliton.

OCIS codes: (320.1590) Chirping; (190.4370) Nonlinear optics, fibers; (190.5530) Pulse propagation and solitons; (190.5650) Raman effect

References and links

1. J. C. Knight, T. A. Birks, P. St. J. Russell, and D. M. Atkin, "All-silica single mode optical fiber with photonic crystal cladding," Opt. Lett. **21**, 1547–1549 (1996).
2. J. K. Ranka, R. S. Windeler, and A. J. Stentz, "Visible continuum generation in air-silica microstructure optical fibers with anomalous dispersion at 800 nm," Opt. Lett. **25**, 25–27 (2000).
3. T. A. Birks, W. J. Wadsworth, and P. St. J. Russell, "Supercontinuum generation in tapered fibers," Opt. Lett. **25**, 1415–1417 (2000).
4. I. Hartl, X. D. Li, C. Chudoba, R. K. Ghanta, T. H. Ko, J. G. Fujimoto, J. K. Ranka, and R. S. Windeler, "Ultrahigh-resolution optical coherence tomography using continuum generation in an air-silica microstructure optical fiber," Opt. Lett. **26**, 608–610 (2001).
5. R. Holzwarth, T. Udem, T. W. Hansch, J. C. Knight, W. J. Wadsworth, and P. St. J. Russell, "Optical frequency synthesizer for precision spectroscopy," Phys. Rev. Lett. **85**, 2264–2267 (2000).
6. I. G. Cormack, D. T. Reid, W. J. Wadsworth, J. C. Knight, and P. St. J. Russel, "Observation of soliton self-frequency shift in photonic crystal fiber," Electron. Lett. **38**, 167–169 (2002).
7. A. B. Fedotov, P. Zhou, Y. N. Kondrat'ev, S. N. Bagayev, V. S. Shevandin, K. V. Dukel'skii, V. B. Smirnov, A. P. Tarasevitch, D. von der Linde, and A. M. Zheltikov, "The mode structure and spectral properties of supercontinuum emission from microstructure fibers," JETP **95**, 851–860 (2002).
8. A. Apolonski, B. Povazay, A. Unterhuber, W. Drexler, W. J. Wadsworth, J. C. Knight, and P. St. J. Russell, "Spectral shaping of supercontinuum in a cobweb photonic-crystal fiber with sub-20-fs pulses," J. Opt. Soc. Am. B **19**, 2165–2170 (2002).
9. K. L. Corwin, N. R. Newbury, J. M. Dudley, S. Coen, S. A. Diddams, K. Weberand, and R. S. Windeler, "Fundamental noise limitations to supercontinuum generation in microstructure fiber," Phys. Rev. Lett. **90**, 113,904 (2003).
10. Z. Zhu and T. G. Brown, "Polarization properties of sumpercontinuum spectra generated in birefringent photonic crystal fibers," J. Opt. Soc. Am. B **21**, 249–257 (2004).
11. K. J. Blow and D. Wood, "Theoretical description of transient stimulated Raman scattering in optical fibers," IEEE J. Quantum Electron. **25**, 2665–2673 (1989).
12. A. L. Gaeta, "Nonlinear propagation and continuum generation in microstructured optical fibers," Opt. Lett. **27**, 924–926 (2002).
13. G. P. Agrawal, *Nonlinear Fiber Optics*, 3rd ed. (Academic, San Diego, 2002).

#3540 - $15.00 US Received 16 December 2003; revised 16 February 2004; accepted 17 February 2004

14. J. M. Dudley and S. Coen, "Coherence properties of supercontinuum spectra generated in photonic crystal and tapered optical fibers," Opt. Lett. **27**, 1180–1182 (2002).
15. Y. Wu, C.-Y. Lou, M. Han, T. Wang, and Y.-Z. Gao, "Effects of pulse chirp on supercontinuum produced in dispersion decreasing fibre," Chin. Phys. **11**, 578–582 (2002).
16. A. V. Husakou and J. Herrmann, "Supercontinuum generation of higher-order solitons by fission in photonic crystal fibers," Phys. Rev. Lett. **87**, 203901 (2001).
17. J. Herrmann, U. Griebner, N. Zhavoronkov, A. Husakou, D. Nickel, J. C. Knight, W. J. Wadsworth, P. St. J. Russell, and G. Korn, "Experimental evidence for supercontinuum generation by fission of higher-order solitons in photonic fibers," Phys. Rev. Lett. **88**, 173901 (2002).
18. J. P. Gordon, "Theory of the soliton self-frequency shift," Opt. Lett. **11**, 662–664 (1986).
19. F. G. Omenetto, B. P. Luce, and A. J. Taylor, "Genetic algorithms pulse shaping for optimum femtosecond propagation in optical fibers," J. Opt. Soc. Am. B **16**, 2005–2009 (1999).

1. Introduction

Photonic crystal fibers (PCFs) [1] have recently attracted a great of interest due to their unusual optical properties. In particular, with the zero-dispersion wavelength (ZDW) shifted to near 800 nm and the high effective nonlinearity due to small core sizes, PCFs are proving to be a promising medium for broadband supercontinuum (SC) generation. An SC covering more than two octaves was successfully generated in a short length of PCF using low-energy 100-fs pulses from a Ti:Sapphire laser [2]. Similar broadband SC have also been demonstrated in tapered optical fibers [3] that have dispersive and nonlinear properties similar to those of PCFs. Such SC sources have found important applications including optical coherence tomography (OCT) [4] and optical frequency metrology [5].

Many numerical and experimental studies have been carried out with the aim of better understanding the underlying mechanisms in the SC process in PCFs. The effects on the SC generation of input pulse properties such as pulse energy, peak power, pulse duration, and central wavelength have been investigated thoroughly. However, to the best of our knowledge, the influence of input pulse chirp on the SC generation in PCFs has not been studied in detail. Frequency chirping of input pulses is not considered in most published theoretical work; a few experimental studies also have limited investigations on the effect of pulse chirp [6, 7, 8, 9], partly due to difficulties in chirp manipulation and characterization and the isolation of chirp from other pulse parameters. Nevertheless, as an important pulse parameter, initial pulse chirp should be considered to well understand the SC process and could be taken advantage to generate desirable SC spectra. In this paper, we present a detailed numerical study on how the input pulse chirp affects the SC generation in PCFs. We find that, in the anomalous regime, positive chirps enhance SC generation while negative chirps suppress SC generation. In particular, there exists an optimal chirp which maximizes the SC bandwidth, corresponding to the formation of only one long-wavelength fundamental soliton.

2. Numerical model

Without considering the polarization coupling [10], we use a generalized scalar nonlinear Schrödinger equation to model the pulse propagation inside the fiber [11, 12]

$$\frac{\partial A}{\partial z} = \sum_{m\geq 2} \frac{i^{m+1}\beta_m}{m!}\frac{\partial^m A}{\partial \tau^m} - \frac{\alpha}{2}A + i\gamma\left(1+\frac{i}{\omega_0}\frac{\partial}{\partial \tau}\right)\left[A(z,\tau)\int_{-\infty}^{\tau} d\tau' R(\tau-\tau')\left|A(z,\tau')\right|^2\right], \quad (1)$$

where A is the electric field amplitude, z is the longitudinal coordinate along the fiber, τ is the time in a reference frame travelling with the pump light, β_m is the mth-order dispersion coefficient at the central frequency ω_0, α is the fiber loss, $\gamma = n_2\omega_0/(cA_{eff})$ is the nonlinear coefficient, $n_2 \simeq 2.0\times 10^{-20}$ m^2/W is the nonlinear refractive index of fused-silica glass, and A_{eff} is the effective mode area of the fiber. This equation allows for modelling the propagation

#3540 - $15.00 US Received 16 December 2003; revised 16 February 2004; accepted 17 February 2004

of pulses with spectral widths comparable to the central frequency ω_0. The response function $R(\tau) = (1 - f_R)\delta(\tau) + f_R h_R(\tau)$ includes both instantaneous electronic and delayed Raman contributions, where $f_R = 0.18$ is the fraction of the Raman contribution to the nonlinear polarization, and $h_R(\tau)$ is the Raman response function of silica fiber, which can be approximated by the expression [11, 13] $h_R(\tau) = (\tau_1^2 + \tau_2^2)/(\tau_1 \tau_2^2) \exp(-\tau/\tau_2) \sin(\tau/\tau_1)$, where $\tau_1 = 12.2$ fs and $\tau_2 = 32$ fs. Eq. (1) is integrated by using the split-step Fourier method [13].

We consider a PCF design which is typical for broadband SC generation near λ = 800 nm. The parameters describe a circular silica rod of diameter of 2.2 μm. The ZDW is $\lambda_D \sim 743$ nm. At a wavelength of 800 nm, the nonlinear coefficient is estimated to be $\gamma \simeq 80$ W^{-1}km^{-1}, and the up to seventh order chromatic dispersion coefficients are β_2 = -1.3504$\times 10^{-2}$ ps^2/m, β_3 = 8.2385$\times 10^{-5}$ ps^3/m, β_4 = -9.1713$\times 10^{-8}$ ps^4/m, β_5 = 1.7589$\times 10^{-10}$ ps^5/m, β_6 = -3.8095$\times 10^{-13}$ ps^6/m, β_7 = 9.4138$\times 10^{-16}$ ps^7/m. The fiber loss is neglected (α = 0) since only a short length of the fiber is considered in the simulations.

The input pulses are assumed to have the form

$$A(0,\tau) = \sqrt{P_0}\,\mathrm{sech}\left(\frac{\tau}{T_0}\right)\exp\left(-i\frac{C_p\tau^2}{2T_0^2}\right), \tag{2}$$

where P_0 is the peak power, T_0 is related to the FWHM by $T_{\mathrm{FWHM}} \approx 1.763 T_0$, and C_p is the parameter representing the initial linear frequency chirp.

3. Numerical results

The effect of initial chirp on the SC bandwidth is shown in Fig. 1(a), which plots the 20-dB SC bandwidth as a function of chirp parameter C_p. The spectrum, temporal intensity and first

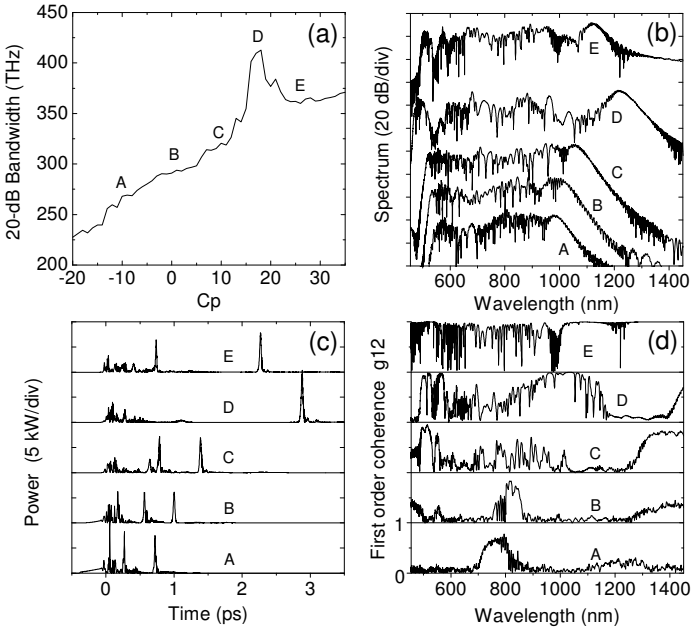

Fig. 1. Effect of chirp on SC: (a) 20-dB bandwidth, (b) temporal shape, (c) spectrum, and (d) coherence. Fiber length L = 10 cm, P_0 = 5 kW, T_0 = 100 fs. Five typical chirps C_p = -10, 0, 10, 17 and 25 are labelled respectively as A, B, C, D and E.

#3540 - $15.00 US Received 16 December 2003; revised 16 February 2004; accepted 17 February 2004

order coherence g_{12} (as defined in Ref. [14]) are also shown in Fig. 1 for five typical chirps of C_p = -10, 0, 10, 17 and 25 (indicated by A, B, C, D and E, respectively). The input pulses have the same peak power P_0 = 5 kW and duration T_0 = 100 fs. In this case, the bandwidth of the input pulse depends on the pre-chirp. Input pulses with larger value of C_p have broader bandwidths. There are several notable features in the figure. First, there is an optimal positive chirp that maximizes the SC bandwidth, as indicated as D; Second, SC bandwidth increases with chirp parameter C_p in an essentially monotonic fashion except near the optimal chirp. We note that, this dependence of SC bandwidth on C_p is quite different from that in dispersion decreasing fibers [15], where the SC bandwidth is reduced by the frequency chirp (both positive and negative). The reason that SC bandwidth increases with C_p can explained as follows. A positive initial chirp adds to the chirp created by SPM near the pulse center, thus enhance the initial pulse compression and get higher peak power, enhancing the SC generation and creating a broader SC spectrum. In contrast, a negative initial chirp reduces the effect of SPM by cancelling the frequency chirps near the pulse center, diminishing the pulse compression and thus creating a narrower SC. It is apparent that the effect of chirping increases with the value of C_p. From another aspect, without considering SPM, a positive initial chirp compresses the pulse initially in the anomalous dispersion regime, while a negative chirp does the opposite. Although this also contributes to the increase of SC bandwidth with C_p, it plays a minor role in the SC generation in PCFs because the nonlinearity (mostly SPM) dominates over dispersion in the initial propagation (i.e., the nonlinear length L_{nl} is much shorter than the dispersion length L_d). In consequence, dramatic spectral broadening takes place within a very short propagation distance as a result of higher-order soliton fission [16, 17]. In our case, L_{nl} = 0.25 cm and L_d = 74 cm. The input pulse completes its dramatic spectral broadening and temporal splitting within a propagation distance less than 3 cm in the case C_p = 0. Therefore, within such a short distance, the contribution of frequency chirping to linear pulse compression is negligible. We also notice that the distance where higher-order soliton fission takes place decreases as C_p increases.

From Fig. 1(b) and (c), we can see clearly how the SC spectrum and temporal intensity change due to different chirps. Except near the optimal chirp, aside from the increase of SC bandwidth with C_p, the longer-wavelength soliton walks off quickly as C_p increases. This is

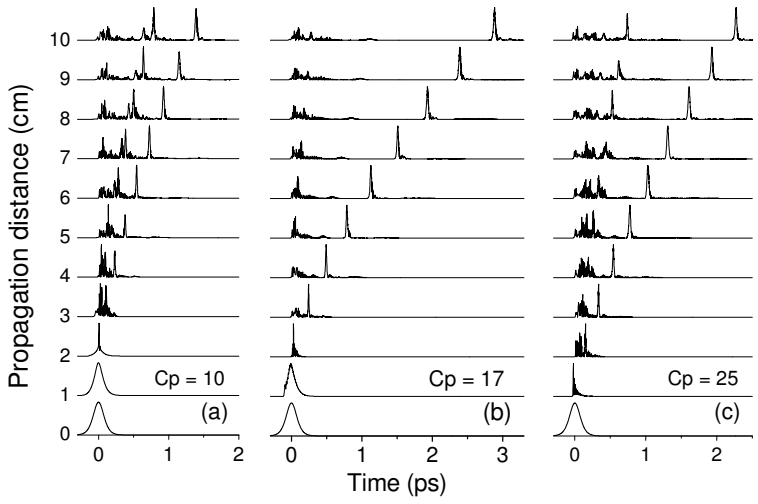

Fig. 2. The temporal evolution along the fiber of the input pulse with initial chirp of (a) C_p = 10, (b) C_p = 17, and (c) C_p = 25. Other simulation conditions are same as in Fig. 1.

#3540 - $15.00 US Received 16 December 2003; revised 16 February 2004; accepted 17 February 2004

expected because a soliton with a longer wavelength has a slower group velocity and thus lags further behind the pump. The first-order coherence of SC shown in Fig. 1(d) was calculated through an ensemble average of 200 simulation pairs by including quantum noise to the input pulse for each simulation [14]. The results show that coherence properties tend to improve as C_p increases, although the effect is only significant for large frequency chirps. The improvement of SC coherence at larger pre-chirps is mainly due to the increase of input bandwidth which makes the added quantum noise less significant in influencing the SC process.

The most interesting effect of chirp is that there exists an optimal positive chirp that maximizes the SC bandwidth. From Fig. 1(b) and (c), we can compare the different characteristics of SC obtained with pulses with chirps near the optimal value. With chirp $C_p \sim 17$, the SC has the maximum bandwidth and only one long-wavelength soliton. In contrast, when the chirp deviates the optimal value, two lower power solitons of different wavelengths (therefore of different group velocities) are formed for both chirps. The SC behavior at the optimal positive chirp is a result of the interplay of the initial phase, SPM, four-wave-mixing (FWM) and stimulated Raman scattering (SRS), which allows for only one single soliton formed with short-wavelength dispersive waves in the spectral broadening process. This scenario can be illustrated by the the pulse evolution along propagation distance in the fiber. Figure 2 shows the SC's temporal behavior along propagation distance for three chirp values of 10, 17 and 25, labelled as points C, D and E in Fig. 1(a). For better visualization, the traces have been normalized. With a positive chirp of 17, the pulse evolves into a single fundamental soliton with part of its energy shed as dispersive waves. In contrast, the pulse with chirp of 10 or 25 evolves into two fundamental solitons, each with lower peak powers and shorter wavelengths than the single soliton case. As expected, the longer wavelength soliton separates faster from the the dispersive waves and also obtains more red-shift due to SRS [18]. We note that, with a large pre-chirp, the bandwidth of the input pulse is broad enough (FWHM $\sim$ 48 THz at C_p = 17 and T_0 = 100 fs) to have significant spectral components within the Raman amplification bandwidth. Therefore, SRS plays an increasingly important role in the initial stage of SC generation and continues to shift the resultant soliton(s) to longer wavelengths. SRS contributes partly to the acceleration of the spectral broadening as C_p increases, as evident in Fig. 2.

Numerical simulations under different pulse parameters such as peak power, pulse duration and center wavelength obtained similar results, with the optimal chirp parameters depending on

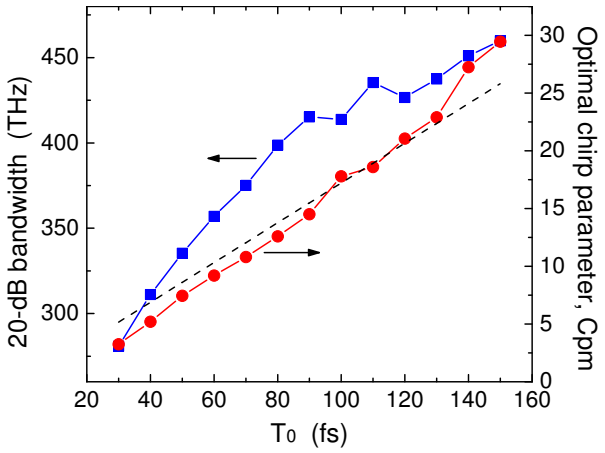

Fig. 3. Calculated optimal chirp and 20-dB SC bandwidth as a function of T_0. The dashed line denotes the soliton order N of the input pulse. Fiber length L = 10 cm, P_0 = 5 kW.

#3540 - $15.00 US Received 16 December 2003; revised 16 February 2004; accepted 17 February 2004

the simulation conditions. For example, we show in Fig. 3 the calculated optimal chirp and corresponding 20-dB SC bandwidth as a function of pulse duration T_0 when the peak power is kept constant at 5 kW. The optimal chirp C_{pm} is basically in direct proportion to T_0. Since the input pulse bandwidth is proportional to C_p/T_0, the input bandwidth at the optimal chirp C_{pm} is almost constant. We also found that, under the simulation condition considered, the optimal chirp C_{pm} follows well the soliton order of the incident pulse $N = (L_d/L_{nl})^{1/2} = (\gamma P_0 T_0^2/|\beta_2|)^{1/2}$, which is also shown in Fig. 3 as the dashed line.

4. Discussion

If the total SC bandwidth is the primary figure-of-merit, the formation of one single fundamental soliton is somewhat more desirable than multiple solitons; the soliton self-frequency shift effect can be taken advantage to get longer wavelength with increasing propagation distance. However, as can be seen in Fig. 1(b), the spectrum at optimal chirp shows more structures than those cases showing multiple soliton excitation. It is clear that multiple different wavelength solitons tend to provide a somewhat flatter spectrum.

In our numerical simulations, we changed the chirp parameter C_p and fixed other parameters (peak power P_0, and pulse duration T_0) in order to observe the effect of C_p. As a result, the bandwidth of the input pulse depends on C_p. Therefore, the observed effect of C_p on the SC generation can also be seen as an input-bandwidth dependent effect. However, this input-bandwidth dependent effect is not simply equivalent to changing the duration of an unchirped pulse, because among other things how the spectral components are arranged to form the input pulse (i.e., pulse chirping) matters. For example, for two pulses that have C_p of opposite signs (see Eq. (2)), although they have the same spectral intensity, the resultant supercontinua are quite different (see Fig. 1).

In view of the usual way by which the pulses are chirped in practice, we also considered the linear chirps obtained by adding quadratic phases to an unchirped input pulse in spectral domain (the pulse energy is conserved). In this case, the most appreciable effect of linear chirping is to broaden the input pulse width and reduce the peak power, resulting in narrower spectra than that from the unchirped pulse. This was also experimentally demonstrated in Ref. [8]. Although smoother SC could be obtained with longer pulses [17], linearly chirping a fixed-energy pulse alone does not seem to be able to achieve both broader and smoother SC. However, more general approaches such as the genetic algorithm pulse shaping techniques (both phase and amplitude shaping) can be used to shape the input unchirped pulses so as to obtain desirable supercontinua [7, 19].

5. Conclusion

In summary, we have numerically studied the effects of initial linear chirp on the SC generated in a photonic crystal fiber. The SC bandwidth is shown to increase with the chirp parameter C_p, and the coherence of SC tends to improve when the initial frequency chirping increases. Interestingly, the simulations show that there exists an optimal chirp value that maximizes the SC bandwidth, corresponding to the formation of a single long-wavelength fundamental soliton. We expect that, as an important parameter, frequency chirping could be used together with other parameters to obtain desirable SC spectra from PCFs.

Acknowledgments

This study was supported in part by a Frank J. Horton fellowship from the Laboratory for Laser Energetics, University of Rochester, and by the National Science Foundation under grant ECS-9816251.

#3540 - $15.00 US Received 16 December 2003; revised 16 February 2004; accepted 17 February 2004